JOURNAL OF MATERIALS SCIENCE 31 (1996) 1991–1996

A study of hydrogen sites in amorphous semiconductors by MuSR–a novel repolarization curve technique

A. SINGH
Department of Physics and Astronomy, Leicester University, Leicester LE1 7RH, UK

Changes in the sites occupied by hydrogen in amorphous silicon with temperature are elucidated for the first time by a new muon implantation (MuSR) technique in which experimental repolarization curves are simulated by groups of theoretical curves, related to each other parametrically. After reviewing MuSR techniques based on repolarization curves, the new parametric method is introduced and applied to amorphous silicon. It reveals that the interstitial (as opposed to bonded) hydrogen moves from sites of higher to lower symmetry as the temperature is raised towards room temperature, and demonstrates significant differences in the behaviour of this interstitial atom between the pure and hydrogenated hosts. The utility of this new analytical technique is demonstrated by combining its results with those of older methods, which yields a fuller picture of hydrogen sites in amorphous silicon than that obtainable from the earlier techniques alone.

1. Introduction

When spin-polarized muons (i.e. muons with spins aligned parallel to each other) are implanted in semiconductors, they bind electrons to form muonium (μ^+e^-) atoms [1]. Information on the state of this exotic atom (e.g. the site it occupies within the atomic matrix of the host material) is obtained by detecting the positron emitted as the muon decays after a mean lifetime of 2.2 μs according to the reaction

$$\mu^+ = e^+ + \nu_e + \bar{\nu}_\mu \qquad (1)$$

where μ^+, e^+, ν_e and $\bar{\nu}_\mu$ are the positive muon, positron, electron neutrino and muon anti-neutrino, respectively. As the muonium atom is chemically very similar to hydrogen [1], it provides a direct method for the modelling of its behaviour in semiconductors.

Several experimental arrangements and analysis techniques are used in the muon implantation studies (MuSR) of polycrystalline and amorphous semiconductors [1, 2]. These may be divided into transverse field (TF) precessional measurements, in which an external field is applied perpendicularly to the muon spin direction, and the longitudinal field (LF) technique, where the muon spin relaxation functions are determined in external fields applied along the spin direction (see Fig. 1).

In the longitudinal field technique, the positron counts (measured as the forward–backward asymmetries, a_0 [2]) provide a measure of the polarization of the muonium spins. This quantity, which is unity for the incident muons (as a consequence of parity non-conservation in beta decays), is spoilt by the hyperfine interaction between the magnetic moments of the muon and electron in the muonium atom, falling to values between zero and 50% [1, 3]. The polarization is progressively recovered in the applied LF field, the rate of recovery depending on the nature of the muonium site (and thus providing a means of identifying this centre). In this paper, a plot of the polarization versus field for a specific muonium centre will be termed its polarization function.

In general, muonium may occupy more than one site in a semiconductor at any time. The experimental data will incorporate information pertaining to all these states, and a consistent methodology must be adopted to resolve these data into the separate components. Two methods of analysis have been used. In the first, the presence of different states is identified by their relaxation rates (i.e. their time rates of decay of polarization) λ_i. The data may thus be separated according to these distinct relaxation rates (usually by fitting the experimental relaxation function with a linear combination of exponential functions, each corresponding to a different λ_i) into components characterized by their λ_i and initial asymmetries, a_{0i} [4]. Plots of the asymmetries, a_{0i}, versus applied field then yield repolarization curves that should correspond to individual muonium centres.

Alternatively, the total initial asymmetry $a_{0T} = \sum_i^n a_{oi}$ may be extracted from the experimental function at the outset, and normalized to yield the total polarization, P_T [5]. A plot of this quantity against the applied field will be referred to as the experimental repolarization curve. As this curve is due to the collective repolarization of all muonium centres in the host, it is clearly equal to the sum of their polarization functions, $P_i(B)$ (which represent the field dependence of their individual polarizations) weighted by their

0022–2461

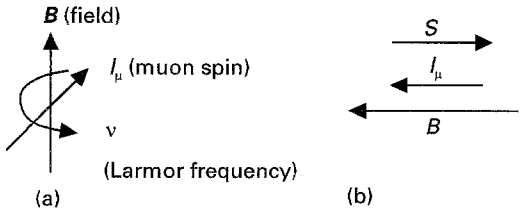

Figure 1 A schematic representation of the muon spin orientation relative to the applied field in the transverse field (TF) and longitudinal field (LF) experimental arrangements. (a) Transverse field – the field B is applied normal to the beam direction (and the perceived muon spin direction I_μ), making the spin precess with the Larmor frequency, ν, about the field direction. (b) Longitudinal field – the field is applied along the muon beam direction, acting to decouple any muon–electron hyperfine coupling. It must be emphasized that the muon spin directions shown here are only schematic. The muon–electron pair actually comprises a spin one system, with four possible spin eigenstates sub-divided into triplet and singlet states.

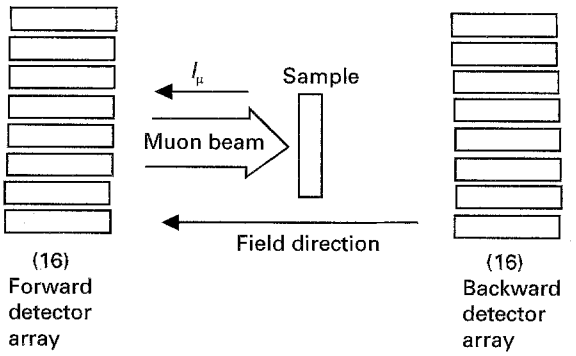

Figure 2 Schematic diagram of the experimental arrangement for the MuSR station at the ISIS facility, Rutherford Appleton Laboratory, Didcot, UK. The "detector arrays" are actually photo-multiplier tubes connected to ZnS detectors via light pipes (not shown) and mounted around large Helmholtz coils providing the applied longitudinal magnetic fields.

relative abundances, F_i (called the muonium fractions). We thus have, in a general case where there are diamagnetic centres (in which the muons experience little or no net magnetic interaction with surrounding electrons) and paramagnetic centres (where there is a sizeable hyperfine interaction between the muon and the surrounding electrons) present

$$P_T(B) = F_d P_D(B) + \sum_i F_i P_i(B) \quad (2)$$

with

$$F_d + \sum_i F_i = 1 \quad (3)$$

where F_d, F_i are the diamagnetic and paramagnetic fractions, respectively, and P_D, $P_i(B)$ the diamagnetic and paramagnetic polarization functions. Two of these functions are always known: $P_D(B)$ is identically equal to unity, and the function for the isotropic paramagnetic muonium is given by [1] :

$$P_{iso}(X) = (\tfrac{1}{2} + X^2)/(1 + X^2) \quad (4a)$$

with

$$X = B/B_o$$

$$B_o = A_{iso}/\gamma_\mu - \gamma_e \quad (4b)$$

where A_{iso} is the isotropic, or contact, hyperfine (hf) constant, and γ_μ, γ_e are the muon and electron gyromagnetic ratios, respectively.

In the case of crystalline semiconductors, there will, in general, be an angular dependence to P_T arising from any anisotropic centre present in the host [1]. We shall confine ourselves here to polycrystalline and amorphous hosts, where this dependence is absent due to the angle-averaging of any anisotropic signal [3, 5].

Equation 2, in principle, may be used to determine the muonium fractions in polycrystalline and amorphous materials once the experimental repolarization curve, $P_T(B)$, has been measured, and the polarization functions, P_i, calculated [5]. In practice, analysis of the amorphous case is made quite difficult by several factors (see Section 3).

Equation 2 also provides a means for modelling the behaviour of the experimental repolarization curve under varying physical conditions such as temperature changes. If the muonium fractions are treated as parameters, then a series of theoretical repolarization curves may be generated by simply varying these values. In the simplest case, one fraction is held fixed while the others varied. Such parametric groups of curves can then be compared to curves obtained experimentally. When used appropriately, this method of data interpretation yields information additional to that obtainable from single curves.

The main objective of this paper is to show how this is possible, and how this technique is able to elucidate qualitative aspects of muonium sites in a-Si not accessible to investigation by other techniques.

The longitudinal field technique of data collection and analysis is briefly outlined and a summary of the use of individual curves to extract information on the muonium states is next given. The parametric curves generally, and type I and II curves in particular, are discussed and the two groups of curves are then applied to the experimental data for pcr-Si, a-Si and a-Si : H taken over a range of temperatures. It is shown how the movement of curves with temperature in a-Si can be interpreted in terms of muonium site changes. This information is then combined with other results to obtain a more complete picture of hydrogen in a-Si than was available previously.

2. The longitudinal field technique – data collection and analysis

In the longitudinal field (LF) technique of MuSR, a magnetic field is applied along the incident muon beam (which is anti-parallel to the muon spin) and the emitted positrons detected in forward and backward detector arrays. Fig. 2 displays schematically the experimental arrangement used in the muon beamlines at the ISIS facility, Rutherford Appleton Laboratory, Didcot.

Counts from the detectors are collected in individual histograms in 16 ns time channels over periods lasting many muon lifetimes. These data are then grouped together into forward $F(t)$ and backward $B(t)$ counts, and are displayed as a histogram of the

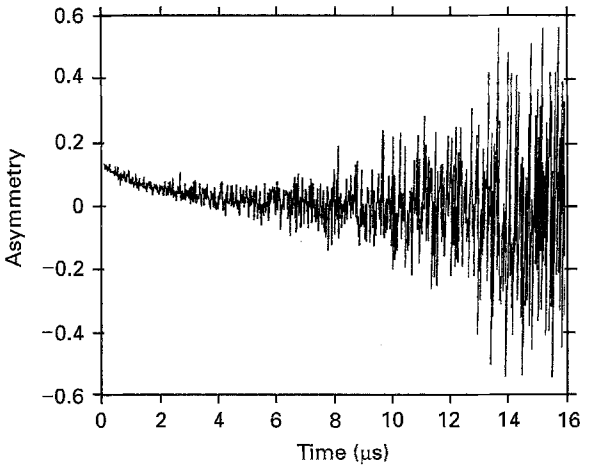

Figure 3 A typical LF histogram collected at the ISIS EMU station. The data are for pcr-Si taken at 175 K for an applied field of 100 G.

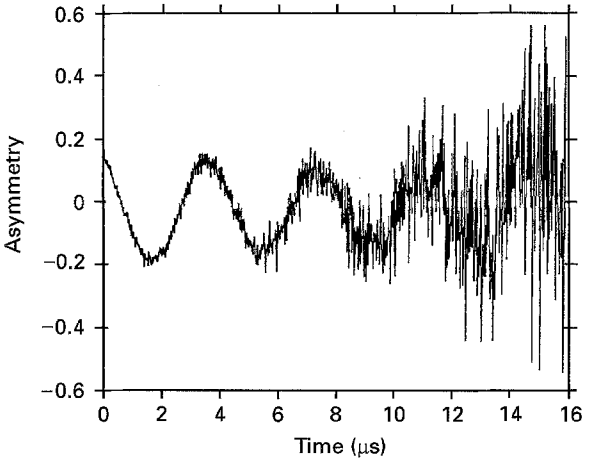

Figure 4 A typical TF histogram collected at the ISIS EMU station at an applied field of 20 G. The oscillations in the signal are due to the precession of the muon spin in the transverse field. The data, which are for a-Si at 300 K, may be used to determine both the alignment factor, α, as well as the diamagnetic fraction, F_d, for the sample.

forward–backward asymmetry, $a(t)$, given by

$$a(t) = \mathbf{a}P(t) = [F(t) - \alpha B(t)]/[F(t) + \alpha B(t)] \quad (5)$$

where **a** is the absolute positron asymmetry at the beam energy used [2], $P(t)$ is the polarization function, and α is an experimental alignment factor. A typical experimental histogram taken in the LF geometry is shown in Fig. 3.

The alignment factor, α, is determined by applying a small (20 G) TF field to the sample. The muons begin to precess in this field at the Larmor frequency, ν given in terms of the applied field, B, by the relation

$$\nu = (\gamma_\mu/2\pi)B \quad (6)$$

Fig. 4 is an example of experimental data exhibiting this precession. The correct value of α is that which produces a total integrated count of zero over an integral number of such oscillations.

At ISIS, the extraction of the initial asymmetry, a_0, and the relaxation rate, λ, from the LF and TF data are conveniently performed by the in-house program UDA.

The repolarization curve data for pcr-Si, a-Si and a-Si : H were collected on the EMU station at ISIS at field points covering the available range of 0–4000 G, and at temperatures ranging between 15 and 300 K.

3. Information from individual decoupling curves

Two paramagnetic centres have been found in the crystalline phases of the tetrahedral group IV elemental semiconductors, including silicon. These are the isotropic, or cage-centre Mu_T (also denoted Mu′, or sometimes simply Mu), and the axially-symmetric, bond-centre Mu_{BC} (frequently labelled Mu*). For these semiconductors, Equation 2 simplifies to

$$P_T(B) = F_d + F_{MuT}P_{MuT}(B) + F_{MuBc}P_{MuBC}(B) \quad (7)$$

with

$$F_d + F_{MuT} + F_{MuBC} = 1 \quad (8)$$

This expression is determined by six parameters. These are the three muonium fractions F_d, F_{MuT} and F_{MuBC}, and the three hf constants belonging to the two paramagnetic centres. To understand what these latter constants are, consider the spin Hamiltonian of the axially symmetric centre. This is given by [6]

$$\boldsymbol{H} = A_{perp}(I_xS_x + I_yS_y) + A_{para}I_zS_z - H_{Zeeman} \quad (9)$$

where A_{perp}, A_{para} are the non-zero elements of the hyperfine tensor

$$\boldsymbol{A} = \begin{bmatrix} A_{perp} & & 0 \\ & A_{perp} & \\ 0 & & A_{para} \end{bmatrix} \quad (10)$$

Instead of these two constants, some workers prefer to use the alternative quantities A_{iso} and $B_{dipolar}$ to define the anisotropic hyperfine tensor. These are related to the former by

$$A_{iso} = 1/3(A_{para} + 2A_{perp}) \quad (11)$$

$$B_{dipolar} = 1/3(A_{para} - A_{perp}) \quad (12)$$

For the isotropic muonium, A_{para} is equal to A_{perp}, yielding the single constant $A_{iso} = A_{para} = A_{perp}$ (with $B_{dipolar} = 0$). Thus there is a total of three hf constants describing the two paramagnetic centres in Equation 7. These may be known, enabling Equation 7 to be used to determine the muonium fractions by a numerical fitting technique [5].

In the case of polycrystalline tetrahedral semiconductors, the polarization function, P_{MuBC}, has been shown to possess a very characteristic feature in the form of a cusp [7] at a field equal to $A_{perp}/(2\gamma_\mu)$. This feature thus provides another means of identifying the anisotropic muonium state in the experimental data.

There are, however, problems that must be resolved before these methods of extracting information from individual repolarization curves can be utilized successfully. The most important is the availability of theoretical calculations for the angle-averaged polarization function $P_{MuBC}(B)$ for the anisotropic muonium Mu_{BC} (i.e. Mu*). This may be calculated numerically

over any field range. For silicon, numerical calculations are available over the experimental range considered here [5]. An analytical expression has also been derived for a generally axially-symmetric centre in the high-field limit [7]. At the time of writing, however, no single result is available that covers the general case over all fields.

A more fundamental problem is encountered in the case of amorphous semiconductors. Here the distribution in bondlengths and cage sizes due to the inherently disordered nature of this phase should introduce spreads in the hf constants. This is most easily understood by considering that the constants are evaluated using the wave-functions of both the host as well as the muonium atom as bases [8]. It is unclear how large this spread is likely to be. As yet, only one attempt has been made to estimate its effect on the repolarization curve [9]. But it seems likely that the large differences seen between the general nature of amorphous and polycrystalline curves (as evident later in a comparison of Fig. 7 with Figs 8 and 9) is due largely to this spread.

4. Parametric curves

The method of parametric curves mentioned in Section 1 can provide useful information which does not depend on the exact knowledge of the hyperfine constants, and therefore has a general validity. In this method, Equation 7 is used to generate theoretical curves parametrically, and to carry out mathematical simulations of groups of related experimental curves. The trends within these curves (rather than the curves themselves) are analysed. They are then associated with changes in the properties of the muonium centres.

The simplest group of these parametric curves is generated by varying the fractions while holding the hf constants fixed. Two particular cases are of special relevance: type I curves, in which the Mu_T fraction, F_{MuT}, is held fixed while F_d is varied, and type II curves in which F_d is fixed while the paramagnetic fractions are varied.

Fig. 5 is an example of the type I group of curves for pcr-Si corresponding to $F_{MuT} = 0.2$. These have been generated with P_{MuT} taken as Equation 4, and P_{MuBC} as calculated numerically by Singh *et al.* [5]. Note the general upward movement of the curves as F_d is increased. An example of type II curves for $F_d = 0.1$ is presented in Fig. 6. These exhibit a more complicated behaviour, the most interesting feature being the two "nodal fields" at which the total polarization is the same regardless of the muonium fractions.

To understand these curves better, consider a change ΔF_{MuBC} such that

$$F'_{MuBC} = F_{MuBC} + \Delta F_{MuBC} \tag{13}$$

and

$$\begin{aligned} P'_T &= F_d + F'_{MuT}P_{MuT}(B) + F'_{MuBC}P_{MuBC}(B) \\ &= F_d + F'_{MuT}P_{MuT}(B) + (F_{MuBC} \\ &\quad + \Delta F_{MuBC})P_{MuBC}(B) \end{aligned} \tag{14}$$

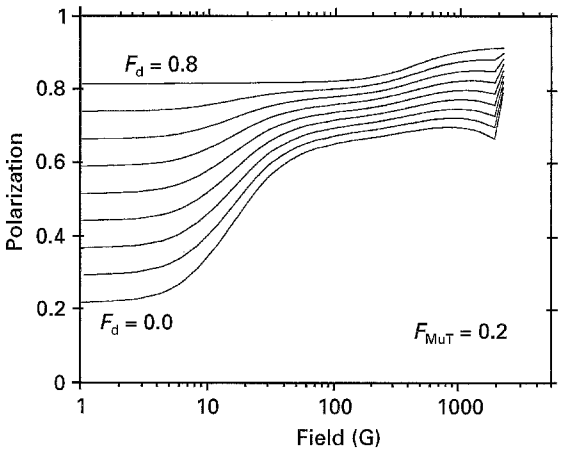

Figure 5 A type I group of parametric curves. These are calculated using the hf constants for silicon, and are for the case where $F_{MuT} = 0.2$.

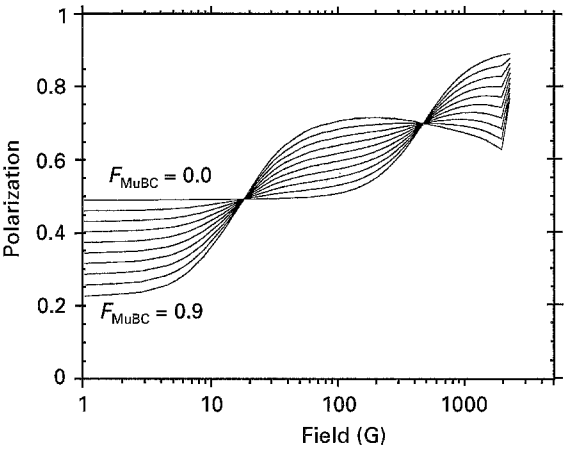

Figure 6 A type II group of parametric curves. These correspond to case of $F_d = 0.1$.

But with F_d fixed

$$F'_{MuT} = F_{MuT} - \Delta F_{MuBC} \tag{15}$$

The change $\Delta P_T = P'_T - P_T$ in P_T brought about by this change in the axially-symmetric muonium fraction is

$$\Delta P_T = \Delta F_{MuBC}[P_{MuBC}(B) - P_{MuT}(B)] \tag{16}$$

There are fields B_1 and B_2 at which the polarization functions are equal. The difference, ΔP_T, between all repolarization curves is therefore identically zero at these fields, yielding the nodal points. We also see that in the field ranges where $P_{MuBC}(B)$ exceeds $P_{MuT}(B)$, an increase in the bond-centre muonium fraction moves the repolarization curve upwards. Where $P_{MuT}(B)$ is greater, however, increasing F_{MuBC} will move the repolarization curve down.

These latter observations prove to be of enormous value in the interpretation of the temperature-dependent behaviour of amorphous repolarization curves.

5. Data simulation – polycrystalline and amorphous silicon

The temperature variation of the experimental repolarization curves of polycrystalline and amorphous

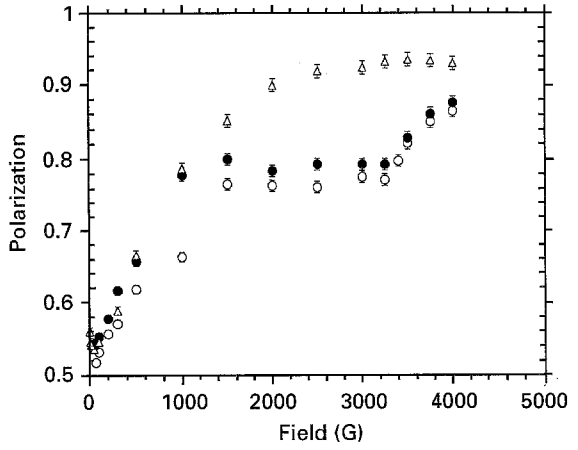

Figure 7 Experimental LF repolarization curves for pcr-Si taken at (○) 15 K, (●) 125 K and (△) 300 K.

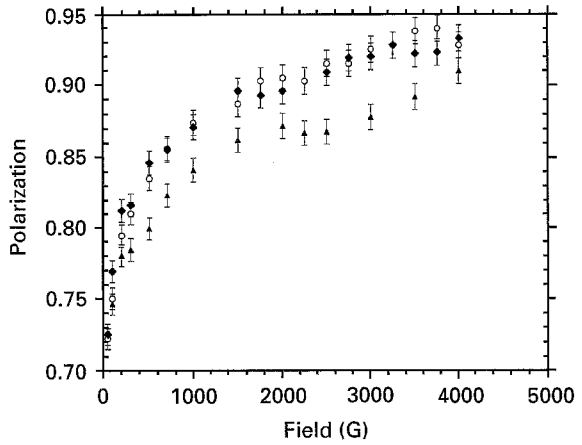

Figure 8 Experimental LF repolarization curves for a-Si taken at (○) 15 K, (◆) 125 K and (▲) 300 K.

silicon hosts form groups of curves related by temperature. The pcr-Si group, shown in Fig. 7, may be simulated by type I parametric curves by noting that in the temperature range 0–300 K of interest here, the anisotropic centre ionizes with increase in temperature, thus increasing the diamagnetic fraction, F_d, while the isotropic muonium fraction, F_{MuT}, remains essentially fixed [1].

Fig. 8 shows the experimental repolarization curves for a-Si taken at three different temperatures. A correspondence between these curves and the parametric curves discussed above is struck by noting that the diamagnetic fraction, F_d, for a-Si and other amorphous semiconductors remains nearly constant over the whole range of temperatures below room temperature [10, 11]. Inasmuch as the relative positions of these experimental curves are determined by changes in the paramagnetic fractions, their temperature-dependent behaviour may be modelled by type II curves. These have been replotted in Fig. 9 on a linear field scale for ease of comparison.

To understand why the two sets of curves look so different, note that the form of P_T in Equation 7 depends on the polarization functions P_{MuT} and P_{MuBC} of the two paramagnetic centres as well as their concentrations. Now the presence of the amorphous counter-

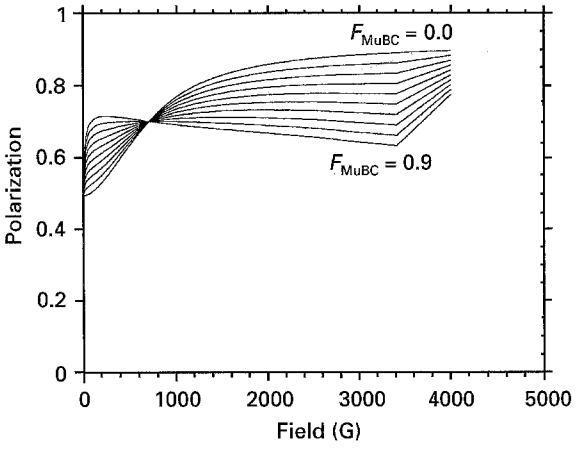

Figure 9 Type II curves re-plotted on a linear scale for ease of comparison with the data for amorphous silicon. $F_d = 0.1$.

parts of both paramagnetic centres have been verified independently [5, 12]. As the effect of the muonium fractions is merely to move the curves relative to each other, the difference between the experimental amorphous curves and the type II curves (which are based on pcr-Si parameters) must thus lie in the polarization functions themselves. These are most likely due to the spread in hf constants mentioned previously, which are expected to "fill in" the sharp Meier cusp of pcr-Si and to make the rise in the curves with field (i.e. repolarization) broader. A possible consequence is that the cross-over of the curves at B1 and B2 becomes less distinguishable in the amorphous case.

6. Muonium site changes in amorphous silicon

The above discussion makes it clear that even in the absence of detailed information on the nature of muonium centres in amorphous semiconductors, type II curves may be used to understand the trends in their repolarization curves. These trends are manifest in (amongst other things) the movement of the curves with temperature.

The curves for a-Si presented in Fig. 8 show a general downward movement as the temperature increases from 15 to 300 K. Inspection of Fig. 9 shows that this can only be due to an increase in the anisotropic muonium fraction. As F_d is fixed, this must be at the expense of the isotropic fraction. This increase in the anisotropic muonium fraction with temperature is supported by the shape of the 300 K curve, which shows a much more pronounced (amorphous) Meier cusp than that at the lower temperatures.

The data thus suggest that in pure amorphous silicon (a-Si), interstitial muonium moves from a more symmetric (e.g. cage-centre) to a less symmetric (e.g. bond-centre) site as the temperature is increased. By analogy, therefore, interstitial hydrogen must undergo site changes from more to less isotropic sites in a-Si, while the concentration of "bonded hydrogen", i.e. hydrogen in deep traps (which is represented here by F_d) remains unchanged.

Although this site change is in keeping with energy calculations [13] which show the bond-centre site to

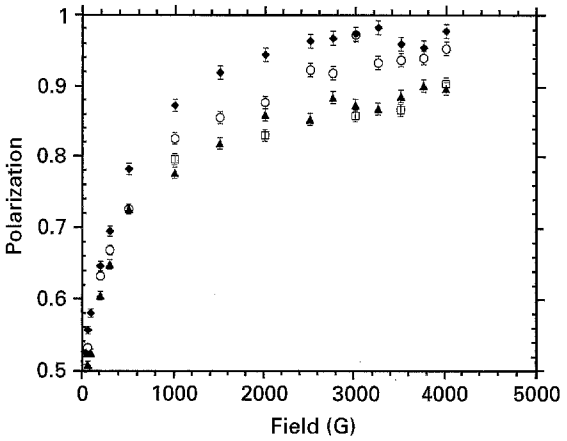

Figure 10 Experimental LF repolarization curves for a-Si:H taken at (○) 15 K, (◆) 125 K, (▲) 300 K and (□) 350 K.

be more stable, this is its first experimental verification for this host. The behaviour is in contrast to that in pcr-Si, where the anisotropic fraction appears to vanish by a temperature of ~200 K [1] while the cage-centre state remains stable to room temperature.

The experimental results for hydrogenated amorphous silicon (a-Si:H), which represents a low-defect system, are presented in Fig. 10. The curves here possess a higher degree of repolarization than for a-Si, consistent with the lower diamagnetic fraction noted here (which remains constant at ~0.4 as compared to 0.6 for a-Si [12]). The amorphous Meier cusp seems to have shifted to higher values, close to that for pcr-Si (3400 G), indicating a correspondingly larger value of ~ -90 MHz for A_{perp}.

The most distinctive feature here, however, is the relative movement of the curves with temperature. Although the curves for the highest temperatures lie lower than the 15 K curve, implying an increase in the anisotropic muonium fraction with temperature, the curve at 125 K is higher. Thus the anisotropic component in this material seems to decrease with temperature before increasing at higher temperatures.

Also interesting is the observation that the 350 K curve stays down. This is in contrast to the result noted previously for a-Si [14]. The rise there was attributed to the ionization of the anisotropic centre. Evidently, this centre is more stable against ionization in the hydrogenated host.

7. Conclusions

1. Modelling experimental data with parametric curves provides a means of gaining insight into the site transformation behaviour of interstitial muonium in amorphous semiconductors without requiring detailed knowledge of the exact nature of the muonium centres involved.

2. This new analysis technique reveals that hydrogen moves from more to less isotropic sites in a-Si as the temperature increases towards room temperature, while the concentrations of bonded hydrogen (as reflected in the value of the diamagnetic fraction) remains essentially fixed.

3. In hydrogenated amorphous silicon (where the defect levels are lower), the anisotropic centre is more like that in pcr-Si to the extent that A_{perp}, is approximately the same. In addition, there seems to be a decrease in the anisotropic fraction prior to an increase as the temperature rises.

Acknowledgements

The author thanks E. A. Davis, Leicester University, for obtaining the funding for this project, and S. F. J. Cox and S. P. Cotrell, ISIS Facility, Rutherford Appleton Laboratory, for their help, guidance and support during the experiments. T. L. Estle, Rice University, is thanked for helpful comments.

References

1. B. D. PATTERSON, *Rev. Mod. Phys.* **60** (1988) 69.
2. S. F. J. COX, *J. Phys. C Solid State Phys.* **20** (1987) 3187.
3. F. L. PRATT, *J. Phys. Condensed Matter* (1995) in press.
4. S. F. J. COX, E. A. DAVIS, W. HAYES, M. C. R. SYMONS, A. WRIGHT, A. SINGH, F. L. PRATT, T. A. CLAXTON and F. JANSEN, *Hyper. Interact.* **64** (1990) 551.
5. A. SINGH, E. A. DAVIS, F. L. PRATT and S. F. J. COX, *ibid.* **86** (1994) 735.
6. B. D. PATTERSON, A. HINTERMANN, W. KUNDIG, P. F. MEIER, F. WALDNER, H. GRAF, E. RECKNAGEL, A. WEIDINGER and Th. WICHERT, *Phys. Rev. Lett.* **40** (1978) 1347.
7. P. F. MEIER, *Hyperf. Interact.* **86** (1994) 723.
8. N. SAHOO, K. C. MISHRA and T. P. DAS *Phys. Rev. Lett.* **55** (1985) 1506.
9. D. W. COOKE, M. LEON, M. A. PACIOTTI, P. F. MEIER, S. F. J. COX, E. A. DAVIS, T. L. ESTLE, B. HITTI, R. L. LICHTI, C. BOEKEMA, J. LAM, A. MORROBEL-SOSA and J. OOSTENS, *Phys. Rev. B.* **50** (1994) 4391.
10. E. A. DAVIS, A. SINGH and S. F. J. COX, *Phil. Trans. R. Soc. Lond.* **350** (1995) 227.
11. A. SINGH and E. MYTILINEOU, (1996) to be published.
12. E. A. DAVIS, A. SINGH, S. F. J. COX, S. R. KREITZMAN, T. L. ESTLE, B. HITTI, R. L. LICHTI, D. LAMP, R. DUVARNEY, D. W. COOKE, M. PACIOTTI and A. C. WRIGHT, *J. Non-Cryst. Solids* **137,138** (1991) 17.
13. C. G. VAN DE WALLE, P. J. H. DENTENER, Y. BARYAM and S. T. PANTELIDES, *Phys. Rev. B.* **39** (1989) 10791.
14. A. SINGH, "Amorphous and Organic semiconductors" Meeting, Chelsea, Spring 1994, Lightfoot Hall, King's College, Manresa Road, Chelsea, London.

Received 22 May
and accepted 7 November 1995